Pion-Kaon Correlations in Central Au + Au Collisions at $\sqrt{s_{NN}} = 130$ GeV

J. Adams,[3] C. Adler,[12] M. M. Aggarwal,[25] Z. Ahammed,[28] J. Amonett,[17] B. D. Anderson,[17] M. Anderson,[5] D. Arkhipkin,[11] G. S. Averichev,[10] S. K. Badyal,[16] J. Balewski,[13] O. Barannikova,[28,10] L. S. Barnby,[17] J. Baudot,[15] S. Bekele,[24] V. V. Belaga,[10] R. Bellwied,[41] J. Berger,[12] B. I. Bezverkhny,[43] S. Bhardwaj,[29] P. Bhaskar,[38] A. K. Bhati,[25] H. Bichsel,[40] A. Billmeier,[41] L. C. Bland,[2] C. O. Blyth,[3] B. E. Bonner,[30] M. Botje,[23] A. Boucham,[34] A. Brandin,[21] A. Bravar,[2] R. V. Cadman,[1] X. Z. Cai,[33] H. Caines,[43] M. Calderón de la Barca Sánchez,[2] J. Carroll,[18] J. Castillo,[18] M. Castro,[41] D. Cebra,[5] P. Chaloupka,[9] S. Chattopadhyay,[38] H. F. Chen,[32] Y. Chen,[6] S. P. Chernenko,[10] M. Cherney,[8] A. Chikanian,[43] B. Choi,[36] W. Christie,[2] J. P. Coffin,[15] T. M. Cormier,[41] J. G. Cramer,[40] H. J. Crawford,[4] D. Das,[38] S. Das,[38] A. A. Derevschikov,[27] L. Didenko,[2] T. Dietel,[12] X. Dong,[32,18] J. E. Draper,[5] F. Du,[43] A. K. Dubey,[14] V. B. Dunin,[10] J. C. Dunlop,[2] M. R. Dutta Majumdar,[38] V. Eckardt,[19] L. G. Efimov,[10] V. Emelianov,[21] J. Engelage,[4] G. Eppley,[30] B. Erazmus,[34] P. Fachini,[2] V. Faine,[2] J. Faivre,[15] R. Fatemi,[13] K. Filimonov,[18] P. Filip,[9] E. Finch,[43] Y. Fisyak,[2] D. Flierl,[12] K. J. Foley,[2] J. Fu,[42] C. A. Gagliardi,[35] M. S. Ganti,[38] T. D. Gutierrez,[5] N. Gagunashvili,[10] J. Gans,[43] L. Gaudichet,[34] M. Germain,[15] F. Geurts,[30] V. Ghazikhanian,[6] P. Ghosh,[38] J. E. Gonzalez,[6] O. Grachov,[41] V. Grigoriev,[21] S. Gronstal,[8] D. Grosnick,[37] M. Guedon,[15] S. M. Guertin,[6] A. Gupta,[16] E. Gushin,[21] T. J. Hallman,[2] D. Hardtke,[18] J. W. Harris,[43] M. Heinz,[43] T. W. Henry,[35] S. Heppelmann,[26] T. Herston,[28] B. Hippolyte,[43] A. Hirsch,[28] E. Hjort,[18] G. W. Hoffmann,[36] M. Horsley,[43] H. Z. Huang,[6] S. L. Huang,[32] T. J. Humanic,[24] G. Igo,[6] A. Ishihara,[36] P. Jacobs,[18] W. W. Jacobs,[13] M. Janik,[39] I. Johnson,[18] P. G. Jones,[3] E. G. Judd,[4] S. Kabana,[43] M. Kaneta,[18] M. Kaplan,[7] D. Keane,[17] J. Kiryluk,[6] A. Kisiel,[39] J. Klay,[18] S. R. Klein,[18] A. Klyachko,[13] D. D. Koetke,[37] T. Kollegger,[12] A. S. Konstantinov,[27] M. Kopytine,[17] L. Kotchenda,[21] A. D. Kovalenko,[10] M. Kramer,[22] P. Kravtsov,[21] K. Krueger,[1] C. Kuhn,[15] A. I. Kulikov,[10] A. Kumar,[25] G. J. Kunde,[43] C. L. Kunz,[7] R. Kh. Kutuev,[11] A. A. Kuznetsov,[10] M. A. C. Lamont,[3] J. M. Landgraf,[2] S. Lange,[12] C. P. Lansdell,[36] B. Lasiuk,[43] F. Laue,[2] J. Lauret,[2] A. Lebedev,[2] R. Lednický,[10] V. M. Leontiev,[27] M. J. LeVine,[2] C. Li,[32] Q. Li,[41] S. J. Lindenbaum,[22] M. A. Lisa,[24] F. Liu,[42] L. Liu,[42] Z. Liu,[42] Q. J. Liu,[40] T. Ljubicic,[2] W. J. Llope,[30] H. Long,[6] R. S. Longacre,[2] M. Lopez-Noriega,[24] W. A. Love,[2] T. Ludlam,[2] D. Lynn,[2] J. Ma,[6] Y. G. Ma,[33] D. Magestro,[24] S. Mahajan,[16] L. K. Mangotra,[16] D. P. Mahapatra,[14] R. Majka,[43] R. Manweiler,[37] S. Margetis,[17] C. Markert,[43] L. Martin,[34] J. Marx,[18] H. S. Matis,[18] Yu. A. Matulenko,[27] T. S. McShane,[8] F. Meissner,[18] Yu. Melnick,[27] A. Meschanin,[27] M. Messer,[2] M. L. Miller,[43] Z. Milosevich,[7] N. G. Minaev,[27] C. Mironov,[17] D. Mishra,[14] J. Mitchell,[30] B. Mohanty,[38] L. Molnar,[28] C. F. Moore,[36] M. J. Mora-Corral,[19] V. Morozov,[18] M. M. de Moura,[41] M. G. Munhoz,[31] B. K. Nandi,[38] S. K. Nayak,[16] T. K. Nayak,[38] J. M. Nelson,[3] P. Nevski,[2] V. A. Nikitin,[11] L. V. Nogach,[27] B. Norman,[17] S. B. Nurushev,[27] G. Odyniec,[18] A. Ogawa,[2] V. Okorokov,[21] M. Oldenburg,[18] D. Olson,[18] G. Paic,[24] S. U. Pandey,[41] S. K. Pal,[38] Y. Panebratsev,[10] S. Y. Panitkin,[2] A. I. Pavlinov,[41] T. Pawlak,[39] V. Perevoztchikov,[2] W. Peryt,[39] V. A. Petrov,[11] S. C. Phatak,[14] R. Picha,[5] M. Planinic,[44] J. Pluta,[39] N. Porile,[28] J. Porter,[2] A. M. Poskanzer,[18] M. Potekhin,[2] E. Potrebenikova,[10] B. V. K. S. Potukuchi,[16] D. Prindle,[40] C. Pruneau,[41] J. Putschke,[19] G. Rai,[18] G. Rakness,[13] R. Raniwala,[29] S. Raniwala,[29] O. Ravel,[34] R. L. Ray,[36] S. V. Razin,[10,13] D. Reichhold,[28] J. G. Reid,[40] G. Renault,[34] F. Retiere,[18] A. Ridiger,[21] H. G. Ritter,[18] J. B. Roberts,[30] O. V. Rogachevski,[10] J. L. Romero,[5] A. Rose,[41] C. Roy,[34] L. J. Ruan,[32,2] V. Rykov,[41] R. Sahoo,[14] I. Sakrejda,[18] S. Salur,[43] J. Sandweiss,[43] I. Savin,[11] J. Schambach,[36] R. P. Scharenberg,[28] N. Schmitz,[19] L. S. Schroeder,[18] K. Schweda,[18] J. Seger,[8] D. Seliverstov,[21] P. Seyboth,[19] E. Shahaliev,[10] M. Shao,[32] M. Sharma,[25] K. E. Shestermanov,[27] S. S. Shimanskii,[10] R. N. Singaraju,[38] F. Simon,[19] G. Skoro,[10] N. Smirnov,[43] R. Snellings,[23] G. Sood,[25] P. Sorensen,[6] J. Sowinski,[13] H. M. Spinka,[1] B. Srivastava,[28] S. Stanislaus,[37] R. Stock,[12] A. Stolpovsky,[41] M. Strikhanov,[21] B. Stringfellow,[28] C. Struck,[12] A. A. P. Suaide,[41] E. Sugarbaker,[24] C. Suire,[2] M. Šumbera,[9] B. Surrow,[2] T. J. M. Symons,[18] A. Szanto de Toledo,[31] P. Szarwas,[39] A. Tai,[6] J. Takahashi,[31] A. H. Tang,[2,23] D. Thein,[6] J. H. Thomas,[18] V. Tikhomirov,[21] M. Tokarev,[10] M. B. Tonjes,[20] T. A. Trainor,[40] S. Trentalange,[6] R. E. Tribble,[35] M. D. Trivedi,[38] V. Trofimov,[21] O. Tsai,[6] T. Ullrich,[2] D. G. Underwood,[1] G. Van Buren,[2] A. M. VanderMolen,[20] A. N. Vasiliev,[27] M. Vasiliev,[35] S. E. Vigdor,[13] Y. P. Viyogi,[38] S. A. Voloshin,[41] W. Waggoner,[8] F. Wang,[28] G. Wang,[17] X. L. Wang,[32] Z. M. Wang,[32] H. Ward,[36] J. W. Watson,[17] R. Wells,[24] G. D. Westfall,[20] C. Whitten, Jr.,[6] H. Wieman,[18] R. Willson,[24] S. W. Wissink,[13] R. Witt,[43] J. Wood,[6] J. Wu,[32] N. Xu,[18] Z. Xu,[2] Z. Z. Xu,[32] A. E. Yakutin,[27] E. Yamamoto,[18] J. Yang,[6] P. Yepes,[30] V. I. Yurevich,[10] Y. V. Zanevski,[10] I. Zborovský,[9] H. Zhang,[43,2] H. Y. Zhang,[17] W. M. Zhang,[17] Z. P. Zhang,[32] P. A. Żołnierczuk,[13] R. Zoulkarneev,[11] J. Zoulkarneeva,[11] and A. N. Zubarev[10]

(STAR Collaboration)*

 0031-9007/03/91(26)/262302(6)$20.00

[1]*Argonne National Laboratory, Argonne, Illinois 60439, USA*
[2]*Brookhaven National Laboratory, Upton, New York 11973, USA*
[3]*University of Birmingham, Birmingham, United Kingdom*
[4]*University of California, Berkeley, California 94720, USA*
[5]*University of California, Davis, California 95616, USA*
[6]*University of California, Los Angeles, California 90095, USA*
[7]*Carnegie Mellon University, Pittsburgh, Pennsylvania 15213, USA*
[8]*Creighton University, Omaha, Nebraska 68178, USA*
[9]*Nuclear Physics Institute AS CR, Řež/Prague, Czech Republic*
[10]*Laboratory for High Energy (JINR), Dubna, Russia*
[11]*Particle Physics Laboratory (JINR), Dubna, Russia*
[12]*University of Frankfurt, Frankfurt, Germany*
[13]*Indiana University, Bloomington, Indiana 47408, USA*
[14]*Insitute of Physics, Bhubaneswar 751005, India*
[15]*Institut de Recherches Subatomiques, Strasbourg, France*
[16]*University of Jammu, Jammu 180001, India*
[17]*Kent State University, Kent, Ohio 44242, USA*
[18]*Lawrence Berkeley National Laboratory, Berkeley, California 94720, USA*
[19]*Max-Planck-Institut für Physik, Munich, Germany*
[20]*Michigan State University, East Lansing, Michigan 48824, USA*
[21]*Moscow Engineering Physics Institute, Moscow, Russia*
[22]*City College of New York, New York City, New York 10031, USA*
[23]*NIKHEF, Amsterdam, The Netherlands*
[24]*The Ohio State University, Columbus, Ohio 43210, USA*
[25]*Panjab University, Chandigarh 160014, India*
[26]*Pennsylvania State University, University Park, Pennsylvania 16802, USA*
[27]*Institute of High Energy Physics, Protvino, Russia*
[28]*Purdue University, West Lafayette, Indiana 47907, USA*
[29]*University of Rajasthan, Jaipur 302004, India*
[30]*Rice University, Houston, Texas 77251, USA*
[31]*Universidade de Sao Paulo, Sao Paulo, Brazil*
[32]*University of Science & Technology of China, Anhui 230027, China*
[33]*Shanghai Institute of Nuclear Research, Shanghai 201800, People's Republic of China*
[34]*SUBATECH, Nantes, France*
[35]*Texas A & M, College Station, Texas 77843, USA*
[36]*University of Texas, Austin, Texas 78712, USA*
[37]*Valparaiso University, Valparaiso, Indiana 46383, USA*
[38]*Variable Energy Cyclotron Centre, Kolkata 700064, India*
[39]*Warsaw University of Technology, Warsaw, Poland*
[40]*University of Washington, Seattle, Washington 98195, USA*
[41]*Wayne State University, Detroit, Michigan 48201, USA*
[42]*Institute of Particle Physics, CCNU (HZNU), Wuhan, 430079 China*
[43]*Yale University, New Haven, Connecticut 06520, USA*
[44]*University of Zagreb, Zagreb, HR-10002, Croatia*

(Received 30 July 2003; published 31 December 2003)

Pion-kaon correlation functions are constructed from central Au + Au STAR data taken at $\sqrt{s_{NN}} = 130$ GeV by the STAR detector at the Relativistic Heavy Ion Collider (RHIC). The results suggest that pions and kaons are not emitted at the same average space-time point. Space-momentum correlations, i.e., transverse flow, lead to a space-time emission asymmetry of pions and kaons that is consistent with the data. This result provides new independent evidence that the system created at RHIC undergoes a collective transverse expansion.

DOI: 10.1103/PhysRevLett.91.262302 PACS numbers: 25.75.Gz, 25.75.Ld

Two-particle correlations for nonidentical particles produced in heavy ion collisions are sensitive to differences in the average emission time and position of the different particle species [1]. Such correlations in data taken at GANIL (^{129}Xe + ^{48}Ti at 45 MeV per nucleon) suggest delayed emission of deuterons with respect to protons [2]. Correlation data from the SPS (Pb-Pb collisions at $\sqrt{s_{NN}} = 17.3$ GeV), and AGS (Au-Au collisions at $\sqrt{s_{NN}} = 4.7$ GeV) also suggest that the pion and proton average space-time emission points do not coincide [2–4]; a partial explanation is that space-momentum correlations arise from the system's collective expansion

[2]. For Au + Au collisions at $\sqrt{s_{NN}} = 130$ GeV, transverse mass spectra, elliptic flow, and deduced pion source radii suggest collective expansion in the transverse plane [5,6]. Such transverse flow may shift the average emission radii of different particle species by different amounts. Also, different species may kinematically decouple from the system at different times depending upon their interaction cross sections [7]. In addition, the average emission time for a given species may be delayed significantly if produced dominantly through resonance decay. We construct pion-kaon correlation functions from Au + Au STAR data taken at $\sqrt{s_{NN}} = 130$ GeV and investigate whether the pions and kaons are emitted at the same average space-time position.

Nonidentical charged particles interact through Coulomb and strong interactions; for the pion-kaon case correlation effects are dominated by the Coulomb interaction. To probe the π-K separation, correlation functions $C(k^*)$ are constructed as the ratio of the k^* distribution constructed with particles from the same event (correlated distribution) divided by the k^* distribution constructed with particles from different events (uncorrelated distribution). k^* is the magnitude of the three-momentum of either particle in the pair rest frame.

For two particles initially moving towards each other the effects of the Coulomb and strong interactions are different from those for two particles initially moving apart. The technique exploits this difference to study emission asymmetries [1,2,8]. Pairs are divided into two groups, which represent either the case where the pions catch up with the kaons or the case where the pions move away from the kaons, depending upon the space-time separation between pion and kaon emission points. Each sample is used to construct two different correlation functions, $C_+(k^*)$ and $C_-(k^*)$, the sign index reflecting the sign of $\vec{v} \cdot \vec{k}^*_\pi$, with $\vec{v}$ the pair velocity and $\vec{k}^*_\pi$ the pion momentum vector in the pair rest frame. If the average space-time emission points of pions and kaons coincide, both correlation functions are identical. If instead, pions are emitted closer to the center of the source than kaons, pions with larger velocity will tend to catch up with kaons, and the Coulomb correlation strength will be enhanced compared to the case where pions are slower than kaons. Hence, the correlation function C_+ will show a larger deviation from unity than C_-. Pairs can be further separated according to the signs of $k^*_{\rm side}$, $k^*_{\rm long}$, and $k^*_{\rm out}$, the $\vec{k}^*_\pi$ projections onto three perpendicular axes in the longitudinally comoving system (LCMS) where the longitudinal component of the pair momentum vanishes [9]. The *out* axis parallels the pair velocity in the LCMS, the *long* axis is the beam axis, and the *side* axis is perpendicular to the other two. $r^*_{\rm out}$, $r^*_{\rm side}$, and $r^*_{\rm long}$ are the corresponding projections of the three-vector $\vec{r}^*$, the relative distance between the particle freeze-out points in the pair rest frame. Because of azimuthal symmetry and symmetry about midrapidity, $\langle r^*_{\rm side}\rangle = \langle r^*_{\rm long}\rangle = 0$. Thus C_+/C_- defined with respect to the signs of $k^*_{\rm side}$ and $k^*_{\rm long}$ must equal unity. If pions and kaons are not emitted at the same average radius in the transverse plane and/or at the same average time, C_+/C_- defined with respect to the sign of $k^*_{\rm out}$ will deviate from unity, unless these two contributions cancel. Thus, one can probe the space-time separation between pion and kaon sources in the transverse plane.

Charged particles are identified and tracked by the STAR Time Projection Chamber (TPC) [10]. This analysis selects the 12% most central collisions, i.e., the events with the largest multiplicity of particles. Selected particles have pseudorapidity $|\eta| < 0.5$. The Au + Au collision point (primary vertex) is required to be within ± 75 cm of the TPC midplane. The noncorrelated pair background is constructed by mixing events whose primary vertices are also separated from each other by less than 10 cm.

Pions and kaons are identified by measuring specific energy loss (dE/dx) in the TPC. When the momentum of pions and kaons exceeds 700 MeV/c, the dE/dx of both species becomes similar which compromises particle identification. In addition, the pion and kaon samples are contaminated by electrons and positrons. The yield of each particle species in the momentum range where the energy losses coincide is interpolated (e^+/e^- contamination) or extrapolated (kaon/pion separation) from the yields measured in the momentum range where there is good separation. In order to quantify the probability of correctly identifying a given species when the dE/dx bands overlap, four probabilities are calculated for each track: the chance that the particle is a π^+ or π^-, K^+ or K^-, p or $\overline{p}$, or e^+ or e^- [6]. To be accepted as a pion or kaon the probability has to be $> 60\%$. Tracks must point back to within 3 cm of the primary vertex; this removes a large number of secondary pions. Pions must have transverse momentum $80\ \text{MeV}/c < p_T < 250\ \text{MeV}/c$ and rapidity $|y| < 0.5$, while kaons must have $400\ \text{MeV}/c < p_T < 700\ \text{MeV}/c$ and $|y| < 0.5$.

Pion-kaon pair identification probability (product of both particle individual dE/dx probabilities) is required to be larger than 60%. Since the e^+-e^- pairs can distort π^--K^+ and π^+-K^- correlation functions, the maximum probability allowed for a given pair to be e^+-e^- is set at 1%, ensuring negligible contribution. Track pairs that share more than 10% of their TPC space points are discarded in order to avoid track merging errors. Two points are defined as shared if the probability of separating hits produced by them in the TPC is less than 99%. After selecting pion-kaon pairs, the correlation functions are constructed by taking the ratio of the k^* distributions of pairs from the same event to the k^* distributions of pairs from different events.

Primary purity and momentum resolution effects are taken into account as described below. Primary purity (P) is the percentage of primary pion-kaon pairs in all

pion-kaon pairs satisfying all cuts. It is estimated to average 77% for unlike-sign pairs and 75% for like-sign pairs. The lower limit for each is 54%. This number is the product of the probability of identifying both pions and kaons using the dE/dx information and the probability of excluding pions and kaons that do not originate from points close to the collision vertex. Excluded pions include decay products of strange hyperons and K_s^0, and pions produced in the detector material. The fraction of secondary pions is estimated from the K_s^0, Λ, and pion yields in Refs. [11–13]. Detector simulations determine the relative reconstruction efficiency of pions from these different sources. Secondary kaons, being rare, are neglected. Assuming that the nonprimary pion-kaon pairs are uncorrelated, the measured correlation function (C_m) is corrected as $C_c(k^*) = [C_m(k^*) - 1]/P(k^*) + 1$. The systematic error introduced by this correction is less than 20%.

The effect of momentum resolution depends upon the correlation function shape. Pion-kaon correlation functions are calculated from the pion and kaon momentum and space-time distributions, accounting for both the Coulomb and strong interactions as in Ref. [14]. The correlation function strength is calculated with the true momentum, while the correlation function is binned as a function of k^* smeared by momentum resolution. Momentum resolution is estimated at the track level by detector simulations. The space-time distribution is chosen so that the main features of the measured correlation function are reproduced. The correction is obtained by comparing correlation functions calculated with and without momentum smearing. The correction enhances $C(k^*)$ by 20% (1%) for $k^* < 5$ MeV/c ($5 < k^* < 10$ MeV/c), first and second bins in Fig. 1, with a conservative systematic error of $\pm 100\%$ on the correction of these two bins.

The top panels of Fig. 1 show the correlation functions for every combination of pion-kaon pairs. The agreement between unlike-sign (π^--K^+ and π^+-K^-) and between like-sign (π^+-K^+ and π^--K^-) correlation functions is excellent. The middle and bottom panels show the ratios C_+/C_- for all pion-kaon pair combinations. C_+/C_- with respect to the sign of $k^*_{\rm side}$ and $k^*_{\rm long}$ is unity within statistical errors in accordance with the requirement that $\langle r^*_{\rm side}\rangle = \langle r^*_{\rm long}\rangle = 0$. However, C_+/C_- with respect to the sign of $k^*_{\rm out}$ is significantly larger than unity at small k^* when the interaction is attractive (π^--K^+ and π^+-K^-) and significantly smaller than unity when the interaction is repulsive (π^+-K^+ and π^--K^-). These results indicate that pions and kaons are not emitted on average at the same radius and/or time.

In order to understand the measured average space-time shift between pion and kaon sources, we compare the data with the RQMD (Relativistic quantum molecular dynamic [15]) model and the blast wave parametrization (BWP) described in Ref. [5]. BWP assumes that the system has undergone longitudinal and transverse expansions, and provides the particle space-time and momentum distributions at kinetic freeze-out. The parameters, system outermost radius $R = 13$ fm, freeze-out proper time $\tau = 93$ m/c, emission duration $\Delta\tau = 0$ fm/c, temperature $T = 110$ MeV, and transverse flow rapidity $\rho(r) = 0.9(r/R)$ (with particle emission radius r) are consistent with fits to pion, kaon, proton, and lambda transverse mass spectra and to pion source radii [5]. The hadronic cascade model, RQMD, also generates transverse flow through rescattering of hadrons [7]. Indeed, turning off hadronic rescattering within this model shuts off transverse flow [16]. In addition, RQMD includes contributions from resonance decay, such as ω, η, and ϕ, which shift pion and kaon emission times.

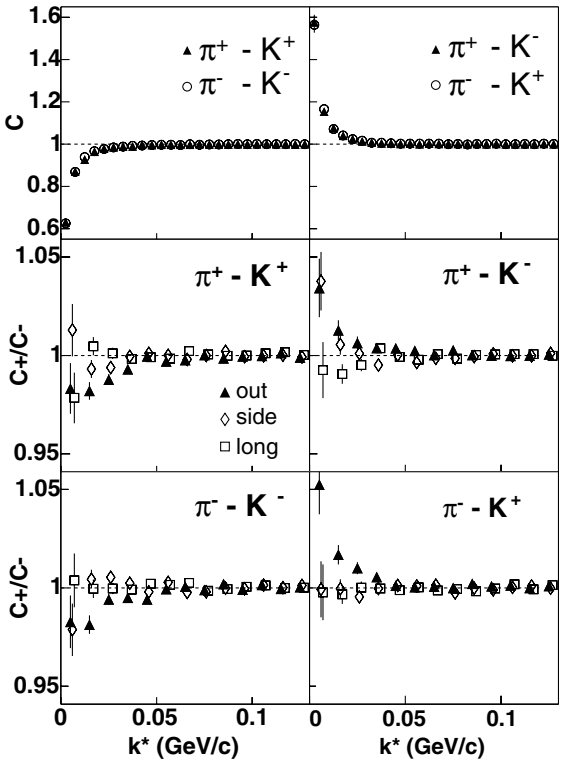

FIG. 1. Top panels: pion-kaon correlation functions $C(k^*)$, the average of $C_+(k^*)$ and $C_-(k^*)$. Middle and bottom panels: ratio of the correlation functions C_+ and C_- defined with the sign of the projections, $k^*_{\rm out}$, $k^*_{\rm side}$, and $k^*_{\rm long}$. Errors are statistical only. The horizontal axis of the ratios C_+/C_- for $k^*_{\rm side}$ ($k^*_{\rm long}$) is shifted by 1 MeV/c (2 MeV/c) to separate the error bars.

Figure 2 shows correlation functions $C(k^*)$ and ratios C_+/C_- obtained from BWP and from RQMD with and without hadronic rescattering. The calculated correlation functions use model space-time and momentum distributions as described in [14], with pion and kaon kinematic cuts chosen to match the data. The correlation functions calculated for like-sign (unlike-sign) pairs are compared to both π^+-K^+ and π^--K^- (π^--K^+ and π^+-K^-) experimental correlation functions, as the calculation depends only on the relative charge of pions and kaons. The small

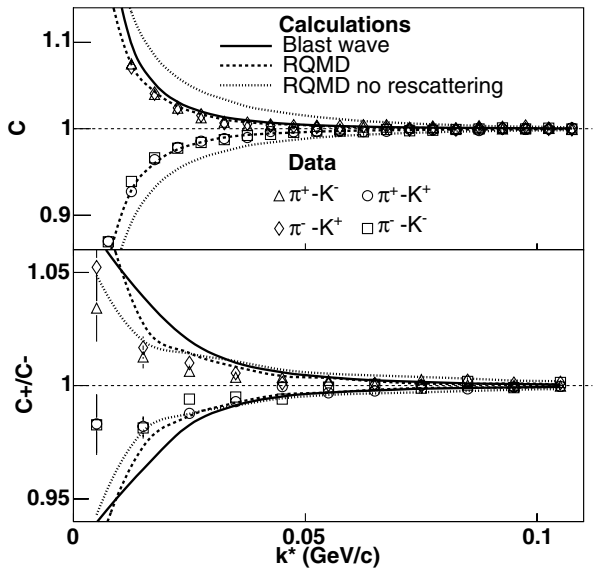

FIG. 2. Comparison of the pion-kaon correlation functions obtained from data and model calculations. Upper panel: $C(k^*)$. Lower panel: $C_+(k^*_{\rm out})/C_-(k^*_{\rm out})$. Model calculations are the lines above 1 for unlike-sign pairs and below 1 for like-sign pairs.

wiggles in the calculated C_+/C_- ratios for $k^* < 20$ MeV/c arise from statistical uncertainties. RQMD and BWP are in qualitative agreement with the measured correlation functions. Turning off rescattering in RQMD leads to a strong correlation, which implies that the pion and kaon sources are too small. On the other hand, RQMD reproduces qualitatively the ratio C_+/C_-.

The effect of source size and source shift is disentangled by simultaneously fitting the correlation functions C_+ and C_-. In order to ensure that the detector acceptance is matched, the particle momenta are taken from experimental pion-kaon pairs constructed by mixing events that pass all the cuts. The particle positions are set such that the distribution of the relative space-time separation between pions and kaons in the pair rest frame is a three-dimensional Gaussian. The free parameters are the Gaussian mean, $\langle\ r^*_{\rm out}\rangle = \langle r^*_{\rm out}(\pi) - r^*_{\rm out}(K)\rangle$ ($\langle\ r^*_{\rm side}\rangle = \langle\ r^*_{\rm long}\rangle = 0$), and the Gaussian width, $\sigma = \sigma_{r^*_{\rm out}} = \sigma_{r^*_{\rm side}} = \sigma_{r^*_{\rm long}}$. Both fit parameters from all four correlation functions are in agreement within statistical errors; combined they give $\sigma = 12.5 \pm 0.4^{+2.2}_{-3}$ fm and $\langle\ r^*_{\rm out}\rangle = -5.6 \pm 0.6^{+1.9}_{-1.3}$ fm with a $\chi^2/{\rm dof} = 134.5/110$. Systematic errors are estimated from the discrepancy between the four correlation functions, the dependence on the input momentum distribution, the uncertainties on primary purity, and the fit range dependence. This -5.6 fm in the pair rest frame becomes in the laboratory frame -3.9 fm (5.4 fm/c) if emission difference is space (time) only.

The parameters σ and $\langle\ r^*_{\rm out}\rangle$ may be extracted directly from BWP or RQMD by constructing the $r^* = \sqrt{(r^*_{\rm out})^2 + (r^*_{\rm side})^2 + (r^*_{\rm long})^2}$ and $r^*_{\rm out}$ distributions. However, neither RQMD nor BWP $\vec{r}^*$ distribution is close to a three-dimensional Gaussian. Thus, to compare models and data fairly, the correlation functions calculated from RQMD and BWP are fitted in exactly the same way as the data. The extracted fit parameters are compared to the data in Table I. The large $\chi^2/{\rm dof}$ values arise because the tails of the $\vec{r}^*$ distributions of RQMD and BWP are not well described by a three-dimensional Gaussian in the pair rest frame. The data appear to be insensitive to these tails due to larger statistical errors.

Consider BWP. At an emission point, the fluid velocity and the thermal velocity in the fluid rest frame combine to give the observed particle velocity $\vec{V}$. If the source did not expand, the relative emission probability for given $\vec{V}$ would track the fireball spatial density. If the source expands but $T = 0$, particles with $\vec{V}$ would come from the single point where the fluid moves with $\vec{V}$. For $T \neq 0$, constant density and unlimited fireball size, the spread of thermal velocity smears this emission point to a nearly spherical volume the size of which increases with decreasing particle mass. This volume must be folded with a realistic fireball spatial density distribution, thereby removing contributions from outside the fireball. Thus, effective centers of emission regions are shifted towards smaller radii for particles of smaller mass. Within our m_t/T range (m_t = transverse mass; $m_t \propto m$ at given V), the relative shift [2] of pions and kaons is significant. There is also an emission time separation: BWP has kinetic freeze-out at fixed longitudinal proper time $\tau = \sqrt{t^2 - z^2}$, so the larger size of the effective pion source yields emission at later laboratory times t. Thus pions are on average emitted closer to the source center and later in time than kaons in agreement with the signs of the departures from unity in the lower two rows of the data in Fig. 1.

In the RQMD model, pion and kaon sources are also spatially shifted when transverse flow builds up by hadronic rescattering. Even when rescattering is turned off, resonance decays delay the pion average emission time and increase the apparent size of the source.

Our results show that pions and kaons are not emitted at the same average space-time position for Au + Au

TABLE I. Fit results using a three-dimensional Gaussian distribution in the pair rest frame. For the data, the first error is statistical and the second systematic. The errors on the model calculations are calculated by rescaling the χ^2 distribution by the minimum value of $\chi^2/{\rm dof}$.

	σ (fm)	$\langle\ r^*_{out}\rangle$ (fm)	$\chi^2/{\rm dof}$
Data	$12.5 \pm 0.4^{+2.2}_{-3}$	$-5.6 \pm 0.6^{+1.9}_{-1.3}$	134.5/110
RQMD	11.8 ± 0.4	-8.0 ± 0.6	205/54
RQMD no rescattering	5.8 ± 0.1	-2.0 ± 0.3	940/54
BWP	9.9 ± 0.1	-6.9 ± 0.3	1020/118

collisions at $\sqrt{s_{NN}} = 130$ GeV. BWP and RQMD are consistent with the data, i.e., with a system whose dominant feature is a transverse collective expansion. These results significantly challenge models that attempt to explain pion, kaon, and proton spectra by purely initial state effects [17,18]. Such an analysis may also be used to probe at what transverse momentum soft processes (expanding system) give way to hard processes since the space-time emission pattern will substantially change at that momentum.

We thank the RHIC Operations Group and RCF at BNL, and the NERSC Center at LBNL for their support. This work was supported in part by the HENP Divisions of the Office of Science of the U.S. DOE; the U.S. NSF; the BMBF of Germany; IN2P3, RA, RPL, and EMN of France; EPSRC of the United Kingdom; FAPESP of Brazil; the Russian Ministry of Science and Technology; the Ministry of Education and the NNSFC of China; SFOM of the Czech Republic; FOM and UU of the Netherlands; DAE, DST, and CSIR of the Government of India; and the Swiss NSF.

*Electronic address: www.star.bnl.gov

[1] R. Lednický, V. I. Lyuboshitz, B. Erazmus, and D. Nouais, Phys. Lett. B **373**, 30 (1996).
[2] R. Lednický, nucl-th/0305027; nucl-th/0112011; nucl-th/0212089.
[3] R. Ganz *et al.*, Nucl. Phys. **A661**, 448 (1999); P. Seyboth *et al.*, Nucl. Phys. (Proc. Suppl.) **B92**, 7 (2001).
[4] E877 Collaboration, D. Miskowiec *et al.*, nucl-ex/9808003.
[5] B. Tomášik, U. Achim Wiedemann, and U. Heinz, Heavy Ion Phys. **17**, 105 (2003); F. Retière and M. Lisa, nucl-th/0312024.
[6] C. Adler *et al.*, Phys. Rev. Lett. **87**, 182301 (2001).
[7] H.W. van Hecke, H. Sorge, and N. Xu, Phys. Rev. Lett. **81**, 5764 (1998).
[8] S. Voloshin, R. Lednický, S. Panitkin, and N. Xu, Phys. Rev. Lett. **79**, 4766 (1997).
[9] R. Lednický, in *Proceedings of the 8th International Workshop on Multiparticle Production, Correlations and Fluctuations* (World Scientific, Singapore, 1998), p. 148; R. Lednický, S. Panitkin, and N. Xu, nucl-th/0304062.
[10] M. Anderson *et al.*, Nucl. Instrum. Methods Phys. Res., Sect. A **499**, 659 (2003).
[11] K. Adcox *et al.*, Phys. Rev. Lett. **88**, 242301 (2002).
[12] C. Adler *et al.*, nucl-ex/0206008.
[13] C. Adler *et al.*, Phys. Rev. Lett. **89**, 092301 (2002).
[14] R. Lednický and V. I. Lyuboshitz, Yad. Fiz. **35**, 1316 (1982) [Sov. J. Nucl. Phys. **35**, 770 (1982)]. FORTRAN program provided by R. Lednický.
[15] H. Sorge, Phys. Rev. C **52**, 3291 (1995).
[16] C. Adler *et al.*, nucl-ex/0306029.
[17] J. Schaffner-Bielich, D. Kharzeev, L. McLerran, and R. Venugopalan, Nucl. Phys. **A705**, 494 (2002); nucl-th/0202054.
[18] NA49 Collaboration, H. G. Fischer *et al.*, Nucl. Phys. **A715**, 118 (2003).